Human NK cells of mice with reconstituted human immune system components require preactivation to acquire functional competence

Strowig, T ; Chijioke, O ; Carrega, P ; Arrey, F ; Meixlsperger, S ; Rämer, P C ; Ferlazzo, G ; Münz, C

Abstract: To investigate human natural killer (NK)-cell reactivity in vivo we have reconstituted human immune system components by transplantation of human hematopoietic progenitor cells into NOD-scid IL2R (null) mice. We demonstrate here that this model allows the development of all NK-cell subsets that are also found in human adult peripheral and cord blood, including NKp46(+)CD56(-) NK cells. Similar to human cord blood, NK cells from these reconstituted mice require preactivation by interleukin-15 to reach the functional competence of human adult NK cells. Mainly the terminally differentiated CD16(+) NK cells demonstrate lower reactivity without this stimulation. After preactivation, both CD16(+) and CD16(-) NK cells efficiently produce interferon- and degranulate in response to stimulation with NK cell-susceptible targets, including K562 erythroleukemia cells. NK-cell lines, established from reconstituted mice, demonstrate cytotoxicity against this tumor cell line. Importantly, preactivation can as well be achieved by bystander cell maturation via poly I:C stimulation in vitro and injection of this maturation stimulus in vivo. Preactivation in vivo enhances killing of human leukocyte antigen class I negative tumor cells after their adoptive transfer. These data suggest that a functional, but resting, NK-cell compartment can be established in immune-compromised mice after human hematopoietic progenitor cell transfer.

DOI: https://doi.org/10.1182/blood-2010-02-270678

Human NK cells of mice with reconstituted human immune system components require pre-activation to acquire functional competence

Till Strowig[1,5&], Obinna Chijioke[2&], Paolo Carrega[3], Frida Arrey[1], Sonja Meixlsperger[2], Patrick C. Rämer[2], Guido Ferlazzo[3,4%] and Christian Münz[1,2%*]

[1]Laboratory of Viral Immunobiology, and Christopher H. Browne Center for Immunology and Immune Diseases, The Rockefeller University, New York, NY

[2]Viral Immunobiology, Institute of Experimental Immunology, University Hospital of Zürich, Zürich, Switzerland

[3]Giannina Gaslini Institute, Genoa, Italy

[4]Laboratory of Immunology and Biotherapy, Department of Human Pathology, University of Messina, Messina, Italy

[5]Present address: Department of Immunobiology, Yale University School of Medicine, New Haven, CT

* Address correspondence to: Christian Münz, Viral Immunobiology, Institute of Experimental Immunology, University Hospital of Zürich, Winterthurerstrasse 190, CH-8057 Zürich, Switzerland, Tel.: +41-44-635-3716, Fax: +41-44-635-6883, e-mail: christian.muenz@usz.ch

[&]These two first authors contributed equally to the work.

[%]These two last authors contributed equally to the work.

Abstract

In order to investigate human NK cell reactivity in vivo we have reconstituted human immune system components by transplantation of human hematopoietic progenitor cells into NOD-scid IL2Rγ^{null} mice. We demonstrate here that this model allows the development of all NK cell subsets that are also found in human adult peripheral and cord blood, including NKp46^{+}CD56^{-} NK cells. Similar to human cord blood, NK cells from these reconstituted mice require pre-activation by IL-15 to reach the functional competence of human adult NK cells. Mainly the terminally differentiated CD16^{+} NK cells demonstrate lower reactivity without this stimulation. After pre-activation, both CD16^{+} and CD16^{-} NK cells efficiently produce IFN-γ and degranulate in response to stimulation with NK cell susceptible targets, including K562 erythroleukemia cells. NK cell lines, established from reconstituted mice, demonstrate cytotoxicity against this tumor cell line. Importantly, pre-activation can as well be achieved by bystander cell maturation via poly I:C stimulation in vitro and injection of this maturation stimulus in vivo. Pre-activation in vivo enhances killing of HLA class I negative tumor cells after their adoptive transfer. These data suggest that a functional, but resting NK cell compartment can be established in immune compromised mice after human hematopoietic progenitor cell transfer.

Introduction

NK cells are innate lymphocytes that are primarily thought to curb viral infections and tumor cell expansion until antigen-specific adaptive immune responses can be primed to eradicate these threats to human health (1). In contrast to adaptive lymphocytes like T and B cells, NK cells recognize their targets through germ line encoded receptors. These receptors transmit either activating or inhibitory signals (2-3). The activating receptors recognize primarily stress induced molecules on infected and transformed cells, including MHC class I like molecules that serve as ligands for the activating NK cell receptor NKG2D, PVR and Nectin-2 as ligands for the activating NK cell receptor DNAM-1, and B7-H6 as well as ligands of still poorly defined identity for the natural cytotoxicity receptors (NCRs) NKp30, NKp46 and NKp44 (4-5). Ligands for these activating receptors are up-regulated upon for example DNA damage or heat shock (6-7), but are also constitutively present on some hematopoietic cells, including myeloid dendritic cells (8), microglia (9) and activated macrophages (10). These activating signals are balanced by inhibitory receptor engagement, recognizing classical and non-classical MHC class I molecules. In humans, killer immunoglobulin-like receptors (KIRs) recognize polymorphic determinants of classical MHC class I molecules, and C-type lectin receptors like the CD94/NKG2 heterodimer engage the non-classical MHC class I molecule HLA-E (11). The balance of transmitted activating and inhibitory signals decides if NK cells will mount effector functions against conjugated target cells.

The main effector characteristics of NK cells are cytokine secretion and cytotoxicity (12), and humans carry NK cell subsets that preferentially mediate one or the other of these functions. $CD56^{bright}CD16^{-}KIR^{-}$ NK cells respond primarily with production of IFN-γ, TNF and GM-CSF to activation, and only exert cytotoxicity after prolonged activation (13). In contrast, $CD56^{dim}CD16^{+}KIR^{+}$ NK cells are constitutively loaded with perforin and granzymes and are the primary human cytotoxic NK cell subset (14). While

the latter population constitutes the majority of peripheral blood NK cells, $CD56^{bright}CD16^{-}KIR^{-}$ NK cells are enriched in human secondary lymphoid organs (15-16). They have been proposed to limit pathogen invasion and polarize adaptive immune responses at these sites (12, 17). Thus cytotoxic NK cells patrol primarily the periphery, while immunoregulatory NK cells support Th1 polarization in secondary lymphoid organs.

The developmental pathways leading to the functionally distinct human NK cell subsets are still being defined (18). So far three alternative pathways have been proposed. Originally, it was proposed that NK cells develop exclusively in the bone marrow from which they populate the periphery as constitutively reactive innate lymphocytes (1). After the discovery that the immunoregulatory human NK cells could acquire phenotypic and functional characteristics of cytotoxic NK cells (19-22), it was proposed that $CD56^{bright}CD16^{-}KIR^{-}$ NK cells could home to secondary lymphoid tissues by virtue of their CD62L and CCR7 expression and mature to $CD56^{bright}CD16^{+}KIR^{+}$ NK cells at these sites (23). Alternatively, $CD56^{bright}CD16^{-}KIR^{-}$ NK cells might also develop directly from $CD34^{+}$ precursors in secondary (24) or primary lymphoid organs (25). In order to shed some more light on the requirements for the development of the human NK cell subsets and their functional competence, we investigated human NK cell compartments reconstituted from $CD34^{+}$ hematopoietic stem and progenitor cells in NOD-scid $IL2R\gamma^{null}$ (hu-NSG) mice in comparison to human cord blood and adult blood NK cells. We describe here that both hu-NSG and cord blood NK cells require pre-activation by monokines to reach functional competence as found in adult peripheral blood, and part of this recruitable activity lies dormant in terminally differentiated $CD16^{+}$ NK cells.

Material and Methods:

Preparation of humanized mice

NOD.Cg-*Prkdc*^{scid} *Il2rg*^{tm1Wjl}/SzJ (NSG) mice were obtained from the Jackson Laboratory (Bar Harbor, ME) and raised under specific pathogen free (SPF) conditions. Human fetal liver was obtained from Advanced Bioscience Resources, CA. The tissue was minced and treated with 2 mg/ml collagenase D (Roche Diagnostics, IN) in HBSS with $CaCl_2$/$MgCl_2$ for 30 minutes at room temperature followed by filtering through 70 μm nylon cell strainers (BD Biosciences, CA). $CD34^+$ human hematopoietic stem and progenitor cells (HPCs) were isolated using the direct CD34 MicroBead Kit (Miltenyi Biotec, CA). 2-5 days old NSG mice were irradiated with 100 cGy and injected intra-hepatically with 1-2 x 10^5 $CD34^+$ HPCs 6 h post irradiation. The mice were bled 10-12 weeks post engraftment and peripheral lymphocytes were analyzed by FACS as described previously (26-27) to check for the reconstitution of the human immune system. Animal protocols were approved by the Institutional Animal Care and Use Committee of the Rockefeller University and the Cantonal Veterinary Office Zürich.

Isolation of blood mononuclear cells

Peripheral blood (PB) from healthy adult volunteers was obtained as part of Institutional Review Board-approved protocols from the New York, Liguria and Zürich Blood Centers. Human cord blood (CB) samples were kindly provided by the Liguria Cord Blood Bank (San Martino Hospital, Genoa, Italy) after delivery of the infant and after prior need for clinical samples had been satisfied. Samples were collected from full term mothers upon their informed consent for research purpose, according to the declaration of Helsinki. Cord blood was processed within 16 h after birth to secure viability of cells. Cord Blood and peripheral blood were diluted 1:4 or 1:2 with PBS, respectively, and mononuclear cells (CBMCs/PBMCs) were isolated by density-gradient centrifugation on

Ficoll/Hypaque. Cells were either directly analyzed or cryopreserved for further analyses. Purified NK cells were obtained by negative selection using NK Cell Isolation Kits (Miltenyi Biotec).

Isolation of cells from tissues of hu-NSG mice

For isolation of cells from spleen and lung, organs were minced and treated with 2 mg/ml collagenase D in HBSS with $CaCl_2$/$MgCl_2$ for 30 minutes at RT followed by filtering through 70 μm nylon cell strainers. Livers of mice were perfused with PBS to remove blood for the isolation of liver-resident cells and subsequently single cell suspensions were generated as described for spleen and lung. Single cell suspensions from lymph nodes were generated by meshing the organs through 70 μm nylon cell strainers. Contaminating erythrocytes in cell suspensions were lysed using ACK lysis buffer or removed by density-gradient centrifugation on Ficoll/Hypaque, and remaining cells were washed, and subjected to subsequent analysis and functional assays. Purified NK cells were obtained by negative selection using NK Cell Isolation Kits, supplemented with anti-mouse CD45 antibodies (Miltenyi Biotec).

Generation of polyclonal NK cell lines

In order to generate polyclonal NK cells from mice with reconstituted human immune system components, murine cells were depleted from splenocytes using anti-mouse CD45 microbeads und human cells were subsequently cultured in medium with 100 IU/ml of IL-2. Cells were split upon becoming confluent and medium was replaced. After two weeks cell cultures contained >95% human NK cells ($hCD45^+NKp46^+$) as analyzed by flow cytometry.

Degranulation assay

To characterize the functional capacities of NK cells within bulk cell populations, we stimulated bulk cells (splenocytes, cord blood mononuclear cells, peripheral blood mononuclear cells, respectively) with target cells at an effector to target ratio of 1:1 for 6 h in the presence of anti-CD107a antibody. To detect spontaneous degranulation and cytokine production, a control without target cells was included. After 1 h, monensin (Sigma-Aldrich, 1µg/ml) was added to all samples. At the end of the incubation, cells were stained on ice with antibodies against human CD45, CD3, and NKp46, washed, fixed, permeabilized, and finally labeled with an anti-IFN-γ antibody. Cells were subsequently analyzed by flow cytometry.

Cytotoxicity assay

To evaluate the cytotoxic activity of NK cells against the K562 target cell line, cytotoxicity assays were performed, as previously described (16). Briefly, target cells were labeled with PKH26 (Sigma-Aldrich), and then incubated with NK cell lines at the indicated effector/target ratios. After 4 h, cells were harvested; TO-PRO-3-iodide, a membrane-impermeable DNA stain, was added to each culture (0.5 µM final concentration); and cells were finally analyzed by flow cytometry. Background and maximum TO-PRO-3-iodide staining were obtained by incubation of target cells with medium and detergent, respectively. The percent specific lysis was calculated as ((% TO-PRO-3-iodide$^+$PKH26$^+$ cells in effector/target cell co-culture - % TO-PRO-3-iodide$^+$PKH26$^+$ cells in medium)/(% TO-PRO-3-iodide$^+$PKH26$^+$ cells in detergent - % TO-PRO-3-iodide$^+$PKH26$^+$ cells in medium) x 100%.

In vivo cytotoxicity assay

LCL721.221 and LCL721.45 were grown in RPMI, 10% FCS and Penicillin/Streptomycin supplemented with L-Glutamine. After labeling with 5 µM CFSE for 10 min at RT, the reaction was stopped by the addition of FCS, cells washed twice in PBS and 5 x 10^6 cells of both lines injected intravenously into the tails of hu-NSG mice either with or without pre-treatment with 50 µg poly I:C by intraperitoneal injection 18h before. Single cell suspensions of recipient spleens were analyzed 12 h post-transfer after being stained with APC-conjugated anti-HLA class I (w6/32, BioLegend) for the presence of CFSE positive cells. Specific lysis was as calculated by gating on CFSE positive cells as (% MHC class I positive - % MHC class I negative) x 100 / % MHC class I positive.

Adoptive transfer of purified NK cell populations

$CD3^-NKp46^+CD56^-$ cells from pooled spleens of hu-NSG mice were sorted to high purity (>98%) on a FACS Aria (BD Biosciences) and labelled with 5 µM CFSE. 1-2 x 10^5 of sorted cells were adoptively transferred into recipient hu-NSG mice (reconstituted with same $CD34^+$ HPCs as donor hu-NSG mice), which were sacrificed 48 h later. Recovered $NKp46^+CFSE^+$ cells from spleens were then analyzed for CD56 expression by flow cytometry.

Monoclonal Antibodies and Flow Cytometry

Analysis of cell surface markers was performed using the following mAbs: V450-conjugated anti-CD45 (clone HI30), FITC- or PerCP-conjugated anti-CD3, APC-conjugated anti-NKp46, PE-Cy7-conjugated anti-CD56, APC-Cy7-conjugated anti-CD16 and FITC- or PE-conjugated anti-CD107a (BD PharMingen, San Diego, CA), FITC-conjugated anti-CD19, PE-conjugated anti-CD158a,h, PE-conjugated anti-CD158b1/b2,j, PE-conjugated anti-CD127 and PE-conjugated anti-NKp46 (Immunotech-Coulter, Fullerton, CA), Alexa Fluor® 647 conjugated anti-CD107a (eBioscence), APC-

conjugated anti-CD56, PE-conjugated CD117, FITC-conjugated anti-CD16 and FITC-conjugated anti-CD3, were from Miltenyi Biotech (Bergisch Gladbach, Germany). The unlabelled anti-NKp46 mAb (clone BAB281) was generously provided by Prof M.C. Mingari's lab. Direct immunofluorescence staining was performed diluting fluorochrome-labeled mAb with 1 mg/mL human γ-globulin (human therapy grade from Biotest S.R.L., Milan, Italy), to block non-specific FcR binding. Cells were then washed and flow cytometric analysis was performed. For indirect immunofluorescence staining, the Alexa Fluor® 633-conjugated isotype specific goat anti-mouse Ab (eBioscence) was used. Negative controls included directly labelled and unlabelled isotype-matched irrelevant mAbs. IFN-γ expression analysis were performed by PE-conjugated reagents (BD Biosciences-PharMingen) or Pacific Blue anti-human IFN-γ antibody (BioLegend, San Diego, CA) after cells were fixed in 2% paraformaldehyde and permeabilized with 0.1% saponin.

Statistical Analysis

Statistical analyses were performed using the Graph-Pad Prism v. 4.00 for Windows (GraphPad Software, San Diego, CA). Statistical significance was evaluated by two-tailed Student t-test.

Results

NOD-scid IL2Rγ^{null} mice reconstitute human NK cells from CD34$^+$ hematopoietic progenitor cells

In order to reconstitute human immune system components in NSG mice, we injected mice neonatally with 10^5 human CD34$^+$ hematopoietic stem and progenitor cells intrahepatically (27-28). After three month we monitored human B cell, T cell, monocyte, dendritic cell and NK cell reconstitution. As previously reported (27) around 60-80% of mononuclear splenocytes were of human origin at this timepoint. Of these 50-60% were B cells, 25-30% were T cells (CD4:CD8 ratio 3:2), 1-2% were plasmacytoid dendritic cells (DCs), 1-2% were conventional DCs, 3-5% were monocytes and 1-3% were NK cells. We decided to characterize the human NK cell distribution further. Compared to spleen, we found higher percentages of CD3$^-$NKp46$^+$ NK cells in lung, blood and liver, while below 1% of mononuclear cells of the bone marrow were NK cells (Figure 1A and B). In lung, the organ with the highest NK cell fraction, up to 7% NK cells were detected. However, when taking total cell numbers for these organs into account, spleen and liver constituted the largest NK cell reservoirs after reconstitution (Figure 1C). These data suggest that human NK cells reconstitute in NSG mice with human immune system components (hu-NSG), and they are present in all strongly blood perfused organs.

Hu-NSG mice and cord blood contain a NKp46$^+$CD56$^-$ NK cell subset

In order to characterize the NK cell subsets that were developing in hu-NSG mice we performed phenotyping of the splenic NK cell compartment. We found KIR, CD94, NKG2D, NKp46, NKG2A and CD16 expression on splenic CD3$^-$CD56$^+$ NK cells (Figure 2A). In comparison to human spleen, whose NK cell compartment is in the majority composed of CD56^{dim}CD16$^+$ NK cells (75%) (16), the minority of hu-NSG derived splenic NK cells belonged to this terminally differentiated subset (25-40%), suggesting a more

immature NK cell compartment in hu-NSG mice compared to human adult spleen. Interestingly, in addition to $CD56^{bright}CD16^{-}$ and $CD56^{dim}CD16^{+}$ NK cells, hu-NSG spleen contained a large subpopulation of $NKp46^{+}CD56^{-}$ NK cells (Figure 2B). Part of these carried in addition to NKp46 other NK cell markers like NKG2A and CD16. Some of the $NKp46^{+}CD56^{-}CD16^{+}$ NK cells expressed KIRs (20-30%), while minimal or no KIR expression was detected on $CD16^{-}$ NK cells (Figure 2C). Vice versa, a subset of $CD3^{-}$ $NKp46^{+}CD56^{-}CD16^{-}$ cells stained positive for CD127 and CD117, and could therefore constitute stage 3 NK cell precursors (29). Since CD56 is up-regulated during human NK cell activation (30), we considered the possibility that the $NKp46^{+}CD56^{-}$ NK cells might be a resting NK cell population prior to a history of pathogen exposure. In order to provide more evidence for this hypothesis, we investigated human cord blood in order to determine if this NK cell subpopulation also existed prior to human pathogen exposure. Indeed, we found within $NKp46^{+}$ cord blood NK cells both CD56 and CD16 negative cells (Figure 2D). The frequency of these $NKp46^{+}CD56^{-}$ NK cells was in contrast very low in adult blood (around 3%). $NKp46^{+}CD56^{-}$ NK cells constituted around 15% of cord blood NK cells amounting in some cord blood samples to up to 30% of the human NK cell compartment (Figure 2E). In order to determine if indeed these $CD3^{-}NKp46^{+}CD56^{-}$ cells can differentiate into $CD3^{-}NKp46^{+}CD56^{+}$ NK cells, we adoptively transferred purified and CFSE labeled $CD3^{-}NKp46^{+}CD56^{-}$ cells into hu-NSG mice reconstituted with autologous $CD34^{+}$ HPCs by intravenous injection. After 48 h, $NKp46^{+}CFSE^{+}$ cells were recovered from recipient spleens and analyzed for their CD56 expression (Figure 2F). All recovered cells had up-regulated CD56. Similarly, $CD3^{-}NKp46^{+}CD56^{-}$ cells from hu-NSG mice up-regulated CD56 after activation in vitro (Supplemental Figure 1). These data suggest that spleens of recently reconstituted hu-NSG mice and human cord blood contains a $NKp46^{+}CD56^{-}$ NK cell population that constitutes around 50% of NK cells in

hu-NSG mice and up to 30% of NK cells in human cord blood, and can differentiate into NKp46^{+}CD56^{+} NK cells in vitro and in vivo.

NK cells from hu-NSG mice have a decreased ability for cytotoxicity and IFN-γ production compared to NK cells from human adults

The functional capacity of NK cells from hu-NSG mice was evaluated by ex vivo stimulation with two NK cell susceptible human target cell lines, the erythroleukemia cell line K562 and the T cell lymphoma line CEM, as well as by monokine stimulation (IL-12+IL15). While K562 is recognized by a combination of NCR, NKG2D and DNAM-1 mediated mechanisms, triggering all NK cell subsets, CEM mediated stimulation of NK cells is primarily mediated by NKG2D and affects mainly CD56^{bright}CD16^{-} NK cells (31). As a surrogate marker for cytotoxicity, degranulation of NK cells in response to these stimuli was assessed by CD107a staining and intracellular IFN-γ staining was monitored as a representative measure for cytokine production (Figure 3A). NK cells from hu-NSG mice degranulated slightly less than human adult peripheral blood NK cells in response to K562 cells. Strikingly, a nearly tenfold difference, was, however, seen in IFN-γ production in response to K562 cells (Figure 3B). Interestingly, NKG2D mediated recognition of CEM was similar between NK cells from hu-NSG mice and human adult blood. When we analyzed K562 recognition by the different NK cell subsets of hu-NSG mice, the functional defect was primarily confined to CD56^{dim} and NKp46^{+}CD56^{-} NK cells (Figure 3C). Similarly, NK cells from cord blood degranulated less efficiently in response to K562 than human adult blood NK cells, and this deficiency was primarily confined to CD56^{dim} and NKp46^{+}CD56^{-} NK cells (Figure 3D). The same NK cell subsets also produced less IFN-γ, when restimulated with K562 cells (data not shown). These data suggest that the resting NK cell compartment of hu-NSG mice degranulate and produce

cytokines less efficiently upon cognate target recognition than human adult NK cells, and part of this deficiency is caused by the $CD56^{dim}$ and $NKp46^{+}CD56^{-}$ NK cell populations.

IL-15 mediated pre-activation can overcome the functional deficiency of NK cells from hu-NSG mice

Since NK cell pre-activation by mature DCs has recently been identified as crucial for full functional capacity of these innate lymphocytes (8, 32-35), we exposed hu-NSG splenocytes to the monokines IL-12 and IL-15 as well as the DC maturing TLR3/mda5 ligand polyinosinic:polycytidylic acid (poly I:C or p(I:C)). Degranulation in response to K562 and CEM was markedly enhanced by IL-15 or poly I:C pre-activation (Figure 4A). In addition, IFN-γ production by hu-NSG NK cells after stimulation with K562 and CEM was boosted five- to tenfold after pre-activation with IL-15 or poly I:C in vitro (Figure 4B). Poly I:C was only able to enhance degranulation and IFN-γ production by NK cells, when bystander cells, presumably mainly DCs, were present, while purified NK cells from hu-NSG mice or cord blood only increased their degranulation and cytokine production in response to K562 after pre-activation with IL-15, but not poly I:C (Figures 4C to F). From these data we conclude that NK cells from hu-NSG mice and cord blood have a similar functional capacity as human adult blood NK cells, but require pre-activation to respond efficiently to cognate target cells, while adult NK cells have a higher constitutive reactivity, possibly due to pre-activation by environmental stimuli.

Pre-activation increases perforin and granzyme B content in NK cells of hu-NSG mice

In addition to the functional parameters of degranulation and IFN-γ production, we also tested if the cytotoxic armament of hu-NSG NK cells increased upon pre-activation in

vitro. For this purpose we stained intracellularly for perforin and granzyme B in $CD3^-$ $NKp46^+$ NK cells of hu-NSG splenocyte cultures that had been exposed to poly I:C or the monokines IL-12 and IL-15. Both IL-15 and poly I:C addition were able to increase the perforin and granzyme B content of hu-NSG mice around fivefold (Supplemental Figure 2A and B). Analogous to the in vitro activation data, the frequency of perforin expressing cells was only increased after IL-15 stimulation of purified splenic NK cells, while poly I:C was not able to induce cytotoxic granules directly (Supplemental Figure 2C). Therefore, pre-activation of NK cells via bystander cell maturation with poly I:C or direct stimulation by IL-15 increases both degranulation capacity and cytotoxic effector molecule expression of NK cells from hu-NSG mice.

Pre-activation boosts degranulation and cytokine production in terminally differentiated NK cells of hu-NSG mice

Since we had noted that primarily $CD56^{dim}$ and $NKp46^+CD56^-$ NK cells of hu-NSG mice and cord blood were functionally deficient in comparison to adult peripheral blood NK cells, we wondered if IL-15 mediated pre-activation would affect these NK cell compartments. We confirmed that these NK cell compartments of hu-NSG mice contained $CD16^+KIR^+$ terminally differentiated human NK cells (Figure 5A and B), and that CD16 expression was not altered on purified NK cells from these subsets during one day of IL-15 activation, while CD56 was up-regulated during this activation period (Supplemental Figure 1 and data not shown). This allowed us to analyze degranulation and cytokine production of $CD16^+$ terminally differentiated hu-NSG NK cells in response to K562 stimulation after IL-15 pre-activation. Indeed, degranulation and IFN-γ production by these NK cells were significantly, around 5 fold, elevated after pre-activation in response to K562 stimulation (Figure 5C and D). In addition, $CD16^-$ NK cells also up-regulated IFN-γ production and degranulation in response to K562 cells after

exposure to IL-15. Thus, the functional deficiency of terminally differentiated NK cells in hu-NSG mice can be overcome by pre-activation with IL-15.

NK cells from hu-NSG mice display cytotoxic function against K562 cells

So far we tested degranulation and cytotoxic molecule expression as surrogate markers for NK cell cytotoxicity of hu-NSG mice. In order to demonstrate cytotoxicity against K562 cells by human reconstituted NK cells from hu-NSG mice directly, we established NK cell lines from hu-NSG mice (Figure 6A). These lines contained to more than 95% $NKp46^+$ NK cells with partial KIR expression. They were comparable or slightly superior to a NK cell lines established from adult human blood with respect to perforin and granzyme B expression. We used the To-Pro-3 incorporation assay as a measurement of direct cytotoxicity (9, 16, 36). The NK cell lines from hu-NSG mice killed K562 with high efficiency of more than 70% lysed cells already at a 10:1 NK:K562 ratio (Figure 6B). This suggests that NK cells from hu-NSG mice are functionally competent, but require cytokine pre-activation to reach their full functional potential.

Poly I:C administration enhances human NK cell functions in vivo

The above described experiments documented the composition and functions of NK cells from hu-NSG mice ex vivo and after activation in vitro. However, in order to assess the capacity of these innate lymphocyte to become functional effectors in vivo, we injected poly I:C intraperitoneally. 18 h after injection, hu-NSG mice were sacrificed and degranulation as well as intracellular IFN-γ content of $CD3^-NKp46^+$ splenocytes was assessed ex vivo or after restimulation with monokines or the NK cell susceptible cell lines K562 and CEM. Already ex vivo, NK cell demonstrated low levels of CD107a staining and intracellular IFN-γ content (Figure 7A, B and C). Moreover, they responded

with three fold better degranulation and five- to tenfold increased IFN-γ production to restimulation with K562 and CEM (Figure 7B and C). In addition, when we adoptively transferred CFSE labeled HLA class I deficient LCL721.221 cells alongside their parental HLA class I positive LCL721.45 cells into hu-NSG mice, LCL721.221 cells were killed in vivo within 12 h, and this cytotoxicity was enhanced by prior poly I:C injection (Figure 7D and E). Cytolysis of LCL721.221 increased from 40 to 85% upon NK cell pre-activation in vivo. These data document that NK cells from hu-NSG mice can be rapidly, within 18 h, pre-activated by poly I:C injection in vivo. This should allow the study of human NK cell functions against viral infections and tumors in vivo in hu-NSG mice.

Discussion

Our study assessed human NK cell reconstitution from $CD34^+$ hematopoietic stem and progenitor cells in NOD-*scid* IL2Rγ^{null} mice (NSG). We found reconstitution of NK cell subsets that are similar to human cord blood, differing by the additional presence of $NKp46^+CD56^-$ NK cells from the subpopulations found in human adult blood. Functionally, these reconstituted NK cell populations also resembled the lower spontaneous NK cell activity found in cord blood, secreting lower levels of IFN-γ and degranulating less efficiently in response to susceptible tumor cell lines like K562. This deficiency was primarily found in terminally differentiated $CD56^{dim}CD16^+$ NK cells, the main cytotoxic NK cell compartment in humans. However, cord blood and reconstituted NSG mouse NK cells could be pre-activated directly with IL-15 or indirectly via poly I:C mediated bystander cell maturation in vitro and in vivo to reach cytotoxicity and cytokine secretion levels similar or exceeding human adult peripheral blood NK cells. These findings suggest that resting NK cells with a similar composition as human cord blood NK cells can be reconstituted in hu-NSG mice, and are functionally competent with respect to mounting NK cell effector functions after pre-activation.

The human NK cell reconstitution in hu-NSG mice is with respect to NK cell subset distribution similar to human NK cell development in BALB/c $Rag2^{-/-}$ $\gamma_c^{-/-}$ mice (22), in which also $NKp46^+CD56^-$, $CD56^{bright}CD16^-KIR^-$and $CD56^{dim}CD16^+KIR^+$ NK cell populations could be observed. Interestingly, however, in all investigated organs except for bone marrow, the frequency of developing NK cells was five- to tenfold lower in reconstituted BALB/c $Rag2^{-/-}$ $\gamma_c^{-/-}$ versus hu-NSG mice (22, 37). This suggests that while NK cell development in the bone marrow progresses to similar levels in these two immunodeficient mouse strains, human NK cells survive and, therefore, accumulate to higher levels in NSG mice. The lower myeloid xenoreactivity mediated by cross-reactivity

of NOD SIRP-α towards human CD47 (38) could be in part responsible for this better NK cell reconstitution. However, human NK cells in BALB/c Rag2$^{-/-}$ $\gamma_c^{-/-}$ mice were able to delay K562 tumor growth in vivo (39) and can be expanded in BALB/c Rag2$^{-/-}$ $\gamma_c^{-/-}$ mice by IL-15 or IL-15/IL-15Rα hybrid molecule administration, reaching then levels of steady-state NK cell reconstitution in NSG mice (22). This expansion occurs at the expense of the CD16 negative NK cell subsets and converts nearly all NK cells to CD16$^+$ partially KIR$^+$ NK cells. A similar NK cell expansion could also be induced in reconstituted NSG mice by hydrodynamic delivery of IL-15 encoding expression plasmids, but the effect on NK cell subset differentiation was not investigated in detail in this study (40). Therefore, we propose that the more efficient NK cell subset reconstitution in hu-NSG mice recommends this model for studying immune responses mediated by these human innate lymphocytes in vivo.

In addition to this essential role of IL-15 for NK cell development and accumulation, which was also previously reported for mouse NK cells (41-42), IL-15 has also been shown to be required for pre-activation of mouse NK cells to reach their full functional potential (35). During viral and bacterial infections this NK cell pre-activation is performed by DCs, possibly via IL-15 trans-presentation (35). Similarly in humans, DCs can activate NK cells to produce cytokines, proliferate and acquire elevated cytotoxicity (8, 32-33, 43-45). Thus reconstituted human NK cells of hu-NSG mice resemble resting NK cells, which like mouse NK cells from animals housed under pathogen free conditions, require pre-activation to become fully functional. In contrast, human adult NK cells display a higher constitutive reactivity, because they are probably partially pre-activated through continuous pathogen encounter. Especially the CD56^{dim}CD16$^+$ NK cells required this pre-activation step, while CD56^{bright}CD16$^-$ NK cells demonstrated already significant reactivity against K562 cells ex vivo, quite similar to CD56^{bright}CD16$^-$

NK cells from human adult blood. These findings are consistent with a previous report, which also suggested that deficiency in NK cell reactivity of human cord blood was primarily confined to $CD56^{dim}CD16^{+}$ NK cells (46). This suggests that primarily terminally differentiated human NK cells require pre-activation. We also identified IL-15 as a potent mediator of human NK cell pre-activation in hu-NSG mice, and poly I:C mediated maturation for NK cell pre-activation probably primarily affected also human DCs to fulfill this function. Indeed, we have previously shown that poly I:C mediated DC maturation renders these cells more efficient in NK cell stimulation than other maturation stimuli (47), and these DCs can interact with both $CD56^{bright}CD16^{-}$ and $CD56^{dim}CD16^{+}$ NK cells to transmit IL-15 dependent signals (48). Thus, hu-NSG mice with reconstituted human immune system compartments should allow studies on resting human NK cells, which are functionally competent.

The functional competence that we observed after pre-activation, also questions further the requirement of NK licensing by somatic tissues for reactivity of this innate lymphocyte subset (49-50). Licensing describes functional competence of NK cells that sequentially up-regulate inhibitory NK cell receptors during development until they express at least one for a self MHC class I molecule. This model is supported by several lines of evidence. Firstly, transgenic expression of an inhibitory receptor decreases the frequency of NK cell expression for other inhibitory receptors, but only in the presence of the cognate MHC class I molecule (51). Secondly, NK cells that do not express self MHC reactive inhibitory receptors are functionally attenuated (52-53). Thirdly, NK cells of TAP deficient patients that do not express MHC class I molecules at high levels on their cell surfaces due to defective peptide loading are functionally compromised (54-55). In contrast, during mouse cytomegalovirus (MCMV) infection, primarily unlicensed NK cells without an inhibitory receptor for polymorphic self MHC class I molecules restrict virus load (50), and unlicensed NK cells acquire functional competence after cytokine

activation (56). Likewise, NK cells lacking inhibitory receptors specific for MHC class I molecules are activated after Listeria monocytogenes infection in vivo, and then produce as much IFN-γ as NK cells carrying these inhibitory receptors (52). Considering these different possibilities, the functional competence of reconstituting human NK cells in hu-NSG mice suggests that licensing can either occur via inhibitory NK cell receptor engagement (CD94/NKG2A or KIR) by HLA class I molecules on reconstituting hematopoietic cells, in addition to previously investigated stromal cells (57), or that unlicensed NK cells can gain similar functionality as licensed human adult blood NK cells after pre-activation in vivo. Further studies on the influence of transgenic HLA class I expression in hu-NSG mice might yield valuable insights into this NK cell development question.

Altogether, our data point towards functional competence of resting human NK cells that develop from $CD34^+$ hematopoietic stem and progenitor cells in hu-NSG mice. We propose that this model could allow the study of NK cell responses during infection with lymphotrophic human pathogens like the Epstein Barr virus (27). These studies could reveal the contribution of NK cells to initial pathogen restriction and priming of protective immune control. Such information could then be harnessed to develop vaccination approaches against human pathogens.

Acknowledgements

We thank the Center for Microscopy and Image Analysis of the University of Zürich for expert technical support and Vinko Tosevski for expert technical advice with flow cytometric cell sorting.

This research was partly supported by grants from the National Cancer Institute (R01CA108609 and R01CA101741), from the Foundation for the National Institutes of Health (Grand Challenges in Global Health) and the Swiss National Science Foundation (310030_126995) to C.M., and by the Assozaizione Italiana per la Ricerca sul Cancro (AIRC) and the Ministero Italiano della Salute, Progetto Strategico Oncologia to G.F. S. M. is a recipient of a post-doctoral fellowship from the German Research Foundation (Deutsche Forschungsgemeinschaft).

Authorship

T.S., O.C., and P.C. performed research; F.A., S.M., and P.R. contributed vital reagents; T.S., O.C., G.F., and C.M. designed research and wrote the manuscript.

Conflict-of-interest disclosure: The authors declare no competing financial interests.

References

1. Trinchieri G. Biology of natural killer cells. *Adv Immunol*. 1989;47:187-376.

2. Lanier LL. NK cell recognition. *Annu Rev Immunol*. 2005;23:225-74.

3. Moretta A, Bottino C, Vitale M, et al. Activating receptors and coreceptors involved in human natural killer cell-mediated cytolysis. *Annu Rev Immunol*. 2001;19:197-223.

4. Brandt CS, Baratin M, Yi EC, et al. The B7 family member B7-H6 is a tumor cell ligand for the activating natural killer cell receptor NKp30 in humans. *J Exp Med*. 2009;206(7):1495-503.

5. Raulet DH. Roles of the NKG2D immunoreceptor and its ligands. *Nat Rev Immunol*. 2003;3(10):781-90.

6. Gasser S, Orsulic S, Brown EJ, Raulet DH. The DNA damage pathway regulates innate immune system ligands of the NKG2D receptor. *Nature*. 2005;436(7054):1186-90.

7. Nice TJ, Coscoy L, Raulet DH. Posttranslational regulation of the NKG2D ligand Mult1 in response to cell stress. *J Exp Med*. 2009;206(2):287-98.

8. Ferlazzo G, Tsang ML, Moretta L, Melioli G, Steinman RM, Münz C. Human dendritic cells activate resting NK cells and are recognized via the NKp30 receptor by activated NK cells. *J Exp Med*. 2002;195(3):343-51.

9. Lünemann A, Lünemann JD, Roberts S, et al. Human NK cells kill resting but not activated microglia via NKG2D- and NKp46-mediated recognition. *J Immunol*. 2008;181(9):6170-7.

10. Nedvetzki S, Sowinski S, Eagle RA, et al. Reciprocal regulation of human natural killer cells and macrophages associated with distinct immune synapses. *Blood*. 2007;109(9):3776-85.

11. Long EO. Negative signaling by inhibitory receptors: the NK cell paradigm. *Immunol Rev*. 2008;224:70-84.

12. Strowig T, Brilot F, Münz C. Noncytotoxic functions of NK cells: direct pathogen restriction and assistance to adaptive immunity. *J Immunol*. 2008;180(12):7785-91.

13. Cooper MA, Fehniger TA, Turner SC, et al. Human natural killer cells: a unique innate immunoregulatory role for the $CD56^{bright}$ subset. *Blood*. 2001;97(10):3146-51.

14. Jacobs R, Hintzen G, Kemper A, et al. $CD56^{bright}$ cells differ in their KIR repertoire and cytotoxic features from $CD56^{dim}$ NK cells. *Eur J Immunol*. 2001;31(10):3121-7.

15. Fehniger TA, Cooper MA, Nuovo GJ, et al. $CD56^{bright}$ Natural Killer Cells are Present in Human Lymph Nodes and are Activated by T cell Derived IL-2: a Potential New Link between Adaptive and Innate Immunity. *Blood*. 2003;102:3052-7.

16. Ferlazzo G, Thomas D, Lin SL, et al. The abundant NK cells in human lymphoid tissues require activation to express killer cell Ig-like receptors and become cytolytic. *Journal of Immunology*. 2004;172:1455-62.

17. Morandi B, Bougras G, Muller WA, Ferlazzo G, Münz C. NK cells of human secondary lymphoid tissues enhance T cell polarization via IFN-gamma secretion. *Eur J Immunol*. 2006;36(9):2394-400.

18. Blom B, Spits H. Development of human lymphoid cells. *Annu Rev Immunol*. 2006;24:287-320.

19. Ferlazzo G, Morandi B, D'Agostino A, et al. The interaction between NK cells and dendritic cells in bacterial infections results in rapid induction of NK cell activation and in the lysis of uninfected dendritic cells. *Eur J Immunol*. 2003;33(2):306-13.

20. Romagnani C, Juelke K, Falco M, et al. $CD56^{bright}CD16^{-}$ killer Ig-like $receptor^{-}$ NK cells display longer telomeres and acquire features of $CD56^{dim}$ NK cells upon activation. *J Immunol*. 2007;178(8):4947-55.

21. Chan A, Hong DL, Atzberger A, et al. CD56^{bright} human NK cells differentiate into CD56^{dim} cells: role of contact with peripheral fibroblasts. *J Immunol*. 2007;179(1):89-94.

22. Huntington ND, Legrand N, Alves NL, et al. IL-15 trans-presentation promotes human NK cell development and differentiation in vivo. *J Exp Med*. 2009;206(1):25-34.

23. Ferlazzo G, Münz C. Natural killer cell compartments and their activation by dendritic cells. *J Immunol*. 2004;172:1333-9.

24. Freud AG, Becknell B, Roychowdhury S, et al. A human CD34^{+} subset resides in lymph nodes and differentiates into CD56^{bright} natural killer cells. *Immunity*. 2005;22(3):295-304.

25. Vosshenrich CA, Garcia-Ojeda ME, Samson-Villeger SI, et al. A thymic pathway of mouse natural killer cell development characterized by expression of GATA-3 and CD127. *Nat Immunol*. 2006;7(11):1217-24.

26. Shultz LD, Lyons BL, Burzenski LM, et al. Human lymphoid and myeloid cell development in NOD/LtSz-scid IL2R gamma null mice engrafted with mobilized human hemopoietic stem cells. *J Immunol*. 2005;174(10):6477-89.

27. Strowig T, Gurer C, Ploss A, et al. Priming of protective T cell responses against virus-induced tumors in mice with human immune system components. *J Exp Med*. 2009;206(6):1423-34.

28. Gurer C, Strowig T, Brilot F, et al. Targeting the nuclear antigen 1 of Epstein Barr virus to the human endocytic receptor DEC-205 stimulates protective T-cell responses. *Blood*. 2008;112:1231-9.

29. Freud AG, Yokohama A, Becknell B, et al. Evidence for discrete stages of human natural killer cell differentiation in vivo. *J Exp Med*. 2006;203(4):1033-43.

30. Münz C, Dao T, Ferlazzo G, De Cos MA, Goodman K, Young JW. Mature myeloid dendritic cell subsets have distinct roles for activation and viability of circulating human natural killer cells. *Blood*. 2005;105:266 - 73.

31. Pende D, Rivera P, Marcenaro S, et al. Major histocompatibility complex class I-related chain a and UL16-binding protein expression on tumor cell lines of different histotypes: Analysis of tumor susceptibility to NKG2D-dependent natural killer cell cytotoxicity. *Cancer Research*. 2002;62(21):6178-86.

32. Gerosa F, Baldani-Guerra B, Nisii C, Marchesini V, Carra G, Trinchieri G. Reciprocal activating interaction between natural killer cells and dendritic cells. *J Exp Med*. 2002;195(3):327-33.

33. Piccioli D, Sbrana S, Melandri E, Valiante NM. Contact-dependent stimulation and inhibition of dendritic cells by natural killer cells. *J Exp Med*. 2002;195(3):335-41.

34. Fernandez NC, Lozier A, Flament C, et al. Dendritic cells directly trigger NK cell functions: cross-talk relevant in innate anti-tumor immune responses in vivo. *Nat Med*. 1999;5(4):405-11.

35. Lucas M, Schachterle W, Oberle K, Aichele P, Diefenbach A. Dendritic cells prime natural killer cells by trans-presenting interleukin 15. *Immunity*. 2007;26(4):503-17.

36. Lee-MacAry AE, Ross EL, Davies D, et al. Development of a novel flow cytometric cell-mediated cytotoxicity assay using the fluorophores PKH-26 and TO-PRO-3 iodide. *J Immunol Methods*. 2001;252(1-2):83-92.

37. Gimeno R, Weijer K, Voordouw A, et al. Monitoring the effect of gene silencing by RNA-interference in human $CD34^{+}$ cells injected into newborn $RAG2^{-/-}$ gamma $common^{-/-}$ mice:Functional inactivation of p53 in developing T cells. *Blood*. 2004;104(13):3886-93.

38. Takenaka K, Prasolava TK, Wang JC, et al. Polymorphism in Sirpa modulates engraftment of human hematopoietic stem cells. *Nat Immunol*. 2007;8(12):1313-23.

39. Kwant-Mitchell A, Pek EA, Rosenthal KL, Ashkar AA. Development of functional human NK cells in an immunodeficient mouse model with the ability to provide protection against tumor challenge. *PLoS ONE*. 2009;4(12):e8379.

40. Chen Q, Khoury M, Chen J. Expression of human cytokines dramatically improves reconstitution of specific human-blood lineage cells in humanized mice. *Proc Natl Acad Sci U S A*. 2009;106(51):21783-8.

41. Kennedy MK, Glaccum M, Brown SN, et al. Reversible defects in natural killer and memory CD8 T cell lineages in interleukin 15-deficient mice. *J Exp Med*. 2000;191(5):771-80.

42. Koka R, Burkett PR, Chien M, et al. Interleukin (IL)-15Rα-deficient natural killer cells survive in normal but not IL-15Rα-deficient mice. *J Exp Med*. 2003;197(8):977-84.

43. Gerosa F, Gobbi A, Zorzi P, et al. The reciprocal interaction of NK cells with plasmacytoid or myeloid dendritic cells profoundly affects innate resistance functions. *J Immunol*. 2005;174(2):727-34.

44. Ferlazzo G, Thomas D, Pack M, et al. Distinct roles of IL-12 and IL-15 in human natural killer cell activation by dendritic cells from secondary lymphoid organs. *Proc Natl Acad Sci U S A*. 2004;101(47):16606-11.

45. Ferlazzo G, Münz C. Dendritic cell interactions with NK cells from different tissues. *J Clin Immunol*. 2009;29(3):265-73.

46. Tanaka H, Kai S, Yamaguchi M, et al. Analysis of natural killer (NK) cell activity and adhesion molecules on NK cells from umbilical cord blood. *Eur J Haematol*. 2003;71(1):29-38.

47. Strowig T, Brilot F, Arrey F, et al. Tonsilar natural killer cells restrict B cell transformation by the Epstein Barr virus via IFN-γ. *PLoS Pathog*. 2008;4(2):e27.

48. Brilot F, Strowig T, Roberts SM, Arrey F, Münz C. NK cell survival mediated through the regulatory synapse with human dendritic cells requires IL-15Rα. *J Clin Invest*. 2007;117(11):3316-29.

49. Kim S, Poursine-Laurent J, Truscott SM, et al. Licensing of natural killer cells by host major histocompatibility complex class I molecules. *Nature*. 2005;436(7051):709-13.

50. Orr MT, Murphy WJ, Lanier LL. 'Unlicensed' natural killer cells dominate the response to cytomegalovirus infection. *Nat Immunol*. 2010;11(4):321-7.

51. Held W, Raulet DH. Ly49A transgenic mice provide evidence for a major histocompatibility complex-dependent education process in natural killer cell development. *J Exp Med*. 1997;185(12):2079-88.

52. Fernandez NC, Treiner E, Vance RE, Jamieson AM, Lemieux S, Raulet DH. A subset of natural killer cells achieves self-tolerance without expressing inhibitory receptors specific for self-MHC molecules. *Blood*. 2005;105(11):4416-23.

53. Anfossi N, Andre P, Guia S, et al. Human NK cell education by inhibitory receptors for MHC class I. *Immunity*. 2006;25(2):331-42.

54. Zimmer J, Donato L, Hanau D, et al. Activity and phenotype of natural killer cells in peptide transporter (TAP)-deficient patients (type I bare lymphocyte syndrome). *J Exp Med*. 1998;187(1):117-22.

55. Vitale M, Zimmer J, Castriconi R, et al. Analysis of natural killer cells in TAP2-deficient patients: expression of functional triggering receptors and evidence for the existence of inhibitory receptor(s) that prevent lysis of normal autologous cells. *Blood*. 2002;99(5):1723-9.

56. Carrega P, Pezzino G, Queirolo P, et al. Susceptibility of human melanoma cells to autologous natural killer (NK) cell killing: HLA-related effector mechanisms and role of unlicensed NK cells. *PLoS ONE*. 2009;4(12):e8132.

57. Roth C, Carlyle JR, Takizawa H, Raulet DH. Clonal acquisition of inhibitory Ly49 receptors on developing NK cells is successively restricted and regulated by stromal class I MHC. *Immunity*. 2000;13(1):143-53.

Figure legends

Figure 1: Distribution of human NK cells in reconstituted NSG mice. Frequency within human CD45 positive cells and total number of $CD3^-NKp46^+$ human NK cells in spleen, blood, lung, liver and bone marrow (BM) of NSG mice reconstituted with human immune system components three month after transfer of $CD34^+$ hematopoietic progenitor cells. Representative flow cytometric staining from one mouse (A) and composite data from 7 mice (B and C) are shown. Numbers in plots represent frequencies within gates.

Figure 2: NK cell subset development in NSG mice in comparison to human adult and cord blood. $CD3^-CD56^+$ human NK cells from spleens of reconstituted NSG mice were analyzed for KIR, CD94, NKG2D, CD16, NKG2A and NKp46 expression (A). One representative of 12 mice is shown. $CD3^-NKp46^+$ human NK cells from spleens of reconstituted NSG mice were analyzed for CD56, CD16 and NKG2A expression (B). A representative staining from one of 12 mice is shown. CD16, KIR, CD127 and CD117 expression on $CD3^-NKp46^+CD56^-$ cells of hu-NSG mice was analyzed (C). One representative out of 3 stainings is displayed. In comparison, CD56 and CD16 expression was analyzed on $CD3^-NKp46^+$ NK cells from human adult (PB) and cord blood (CB). One representative example (D) and composite data (E) of 8 experiments are shown. CFSE labeled $CD3^-NKp46^+CD56^-$ cells of hu-NSG mice were adoptively transferred into hu-NSG mice, which had been reconstituted with autologous $CD34^+$ HPCs. CD56 expression on the recovered $NKp46^+$ CFSE labeled cells from recipient spleens was analyzed after 48 h by flow cytometry (F). Gray shaded histogram of post-sort $CD3^-NKp46^+CD56^-$ cells in comparison to black histogram of post-sort $CD56^+$ (left panel). White histogram of recovered cells in comparison to gray shaded histogram of

cells that were transferred (right panel). One representative of 2 experiments is shown. Numbers in plots represent frequencies within gates or quadrants.

Figure 3: Functional activity of human NK cells from reconstituted NSG mice in comparison to human adult or cord blood NK cells. Degranulation, a surrogate marker for cytotoxicity, and cytokine production were assessed by surface CD107a and intracellular IFN-γ staining in response to ex vivo stimulation with medium, the erythroleukemia cell line K562, the T cell lymphoma cell line CEM and the monokines IL-12 plus IL-15 (IL-12/15). One representative staining (A) and composite data (B) of 12 mice in three experiments are shown. In the composite data human NK cell reactivity of reconstituted NSG spleens was compared to three adult PBMC samples. In addition, the function of the human NK cell subsets $CD56^{bright}CD16^{-}$, $CD56^{dim}CD16^{+}$ and $NKp46^{+}CD56^{-}$ from human adult (PBMC), hu-NSG (C) mice or cord blood (CBMC in D) were compared for degranulation. Composite data of 3 (C) and 6 (D) experiments are shown. Numbers in plots represent frequencies within gates.

Figure 4: Pre-activation enhances human NK cell function in spleen cells from reconstituted NSG mice and human cord blood. Splenocytes from reconstituted NSG mice (A and B) purified NK cells from hu-NSG mice (C and D) and human cord blood (E and F) were used untreated (Medium) or pre-activated with poly I:C (p(I:C)) or the monokines IL-12 and IL-15. These cultures were restimulated with medium alone, monokines, K562 cells or CEM cells. Degranulation (CD107a; A, C and E) and cytokine production (IFN-γ; B, D and F) were evaluated after gating on NKp46 positive cells. A and B represent composite data from 4 mice in two experiments, and C and D from 10 mice in two experiments and E and F from 3 experiments.

Figure 5: Terminally differentiated CD16$^+$ NK cells acquire functional capacity after IL-15 mediated pre-activation. Distribution of KIR$^+$ (A) and CD16$^+$ (B) NK cells in splenic CD56^{bright}, CD56^{dim} and CD56$^-$ NK cell subsets of hu-NSG mice, as gated in the upper panels of (A) in comparison to isotype control staining or (B) staining on marker negative CD3$^+$ cells (gray shaded histograms). Degranulation (C) and IFN-γ production (D) of unstimulated and pre-activated CD16$^+$ and CD16$^-$ NK cells after co-culture with K562 cells were analyzed. A representative experiment of 2 is shown in A and B, while C and D represent composite data of 2 independent experiments. Numbers in plots represent frequencies within gates or marker regions.

Figure 6: Cytotoxic ability of a human NK cell line from reconstituted NSG mice. (A) Comparison of NKp46, KIR, perforin and granzyme B (GrzB) expression of a reconstituted mouse derived human NK cell line with a line of human adult peripheral blood NK cells. (B) Cytotoxicity of the human NK cell line from reconstituted NSG mice against K562. Loss of membrane integrity of PKH26 labelled K562 cells as a measure of cytotoxicity was assessed by To-Pro-3 iodide staining of DNA, which is blocked by intact cell membranes. Cytotoxicity was evaluated at the indicated NK:K562 (E:T) ratios. One representative of 6 experiments with three different NK cell lines from three mice is shown. Numbers in plots represent frequencies within gates.

Figure 7: Pre-activation of human NK cells of reconstituted NSG mice in vivo. Splenocytes of untreated or poly I:C (p(I:C)) injected reconstituted NSG mice were restimulated ex vivo with medium alone or the monokines IL-12 and IL-15, or K562 cells, or CEM cells. Both degranulation (B) and cytokine production (IFN-γ; A and C) were

evaluated. One representative of two experiments (A) and composite data (B) from eight mice are shown. CFSE labeled LCL721.221 (HLA class I negative) and LCL721.45 (HLA class I positive) cells were injected intravenously into untreated or poly I:C pre-activeted hu-NSG mice. 12 h later the composition of CFSE labeled cells in the recipient spleens was analyzed by w6/32 (anti-HLA class I) staining. Analysis of HLA class I expression and CFSE prior to adoptive transfer (D) and after recovery after gating on $CFSE^{+}$ cells (E). One representative out of 3 experiments is shown. Numbers in plots represent frequencies within gates or marker regions.

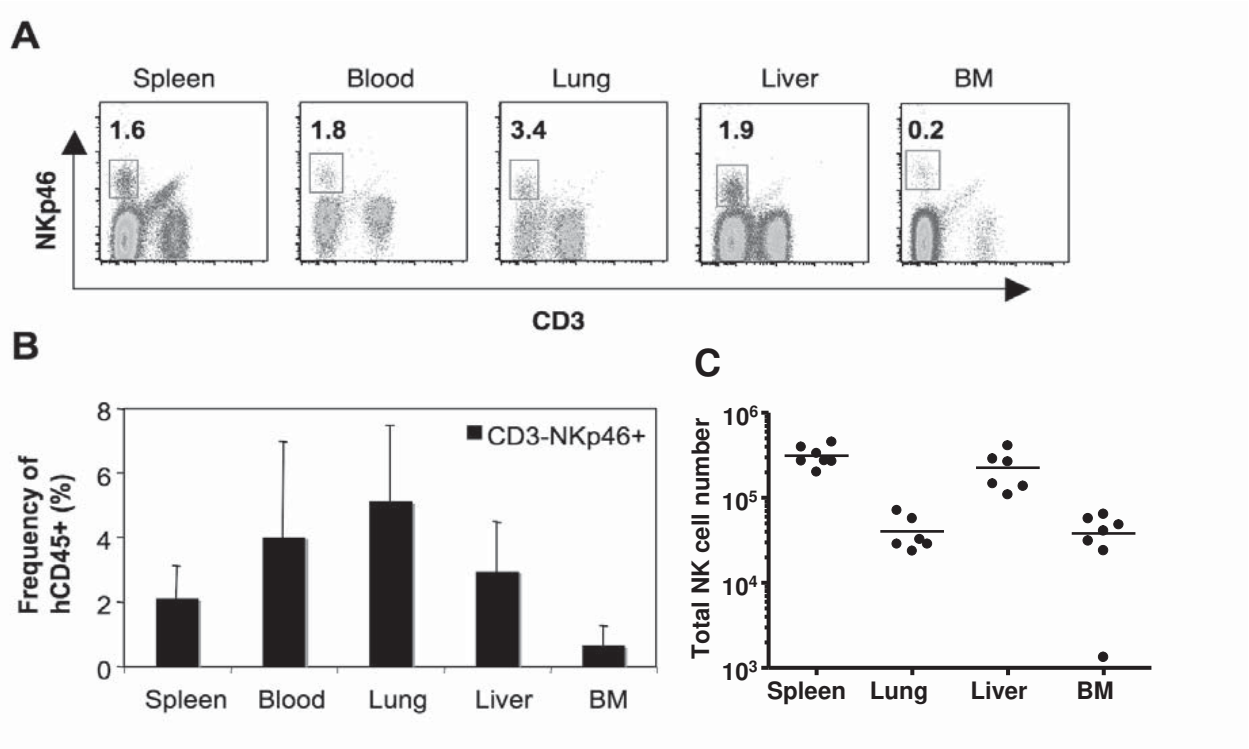
A
Spleen
Blood
Lung
Liver
BM
1.6
1.8
3.4
1.9
0.2
NKp46
CD3
B
Frequency of hCD45+ (%)
CD3-NKp46+
Spleen
Blood
Lung
Liver
BM
C
Total NK cell number
Spleen
Lung
Liver
BM

Figure 1

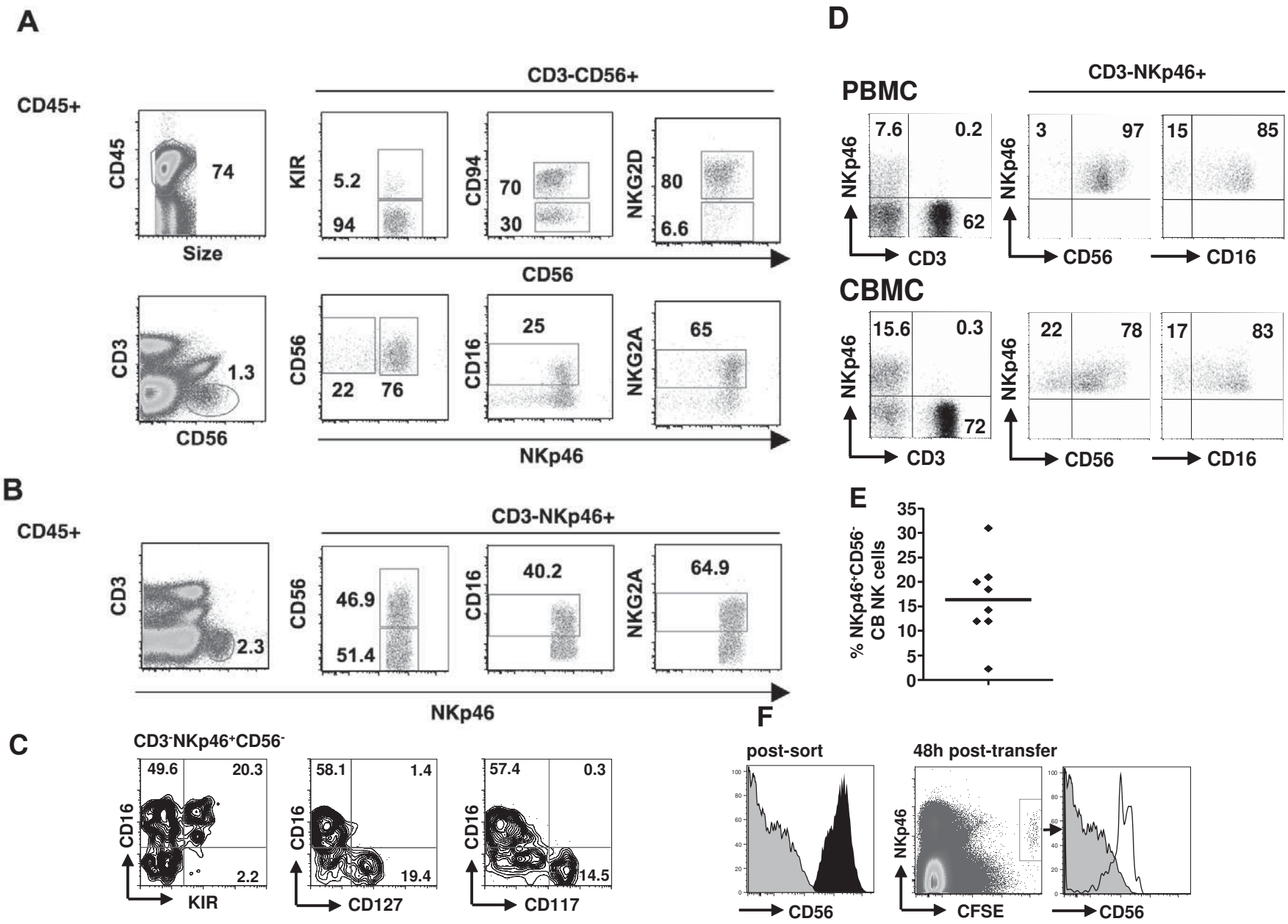
A
CD45+
CD45
74
Size
CD3-CD56+
KIR
5.2
94
CD94
70
30
NKG2D
80
6.6
CD56
CD3
1.3
CD56
22
76
CD16
25
NKG2A
65
NKp46
B
CD45+
CD3-NKp46+
CD3
2.3
CD56
46.9
51.4
CD16
40.2
NKG2A
64.9
NKp46
C
CD3-NKp46+CD56-
CD16
49.6
20.3
2.2
KIR
CD16
58.1
1.4
19.4
CD127
CD16
57.4
0.3
14.5
CD117
D
PBMC
CD3-NKp46+
NKp46
7.6
0.2
62
CD3
NKp46
3
97
15
85
CD56
CD16
CBMC
NKp46
15.6
0.3
72
CD3
NKp46
22
78
17
83
CD56
CD16
E
% NKp46+CD56- CB NK cells
35
30
25
20
15
10
5
0
F
post-sort
CD56
48h post-transfer
NKp46
CFSE
CD56

Figure 2

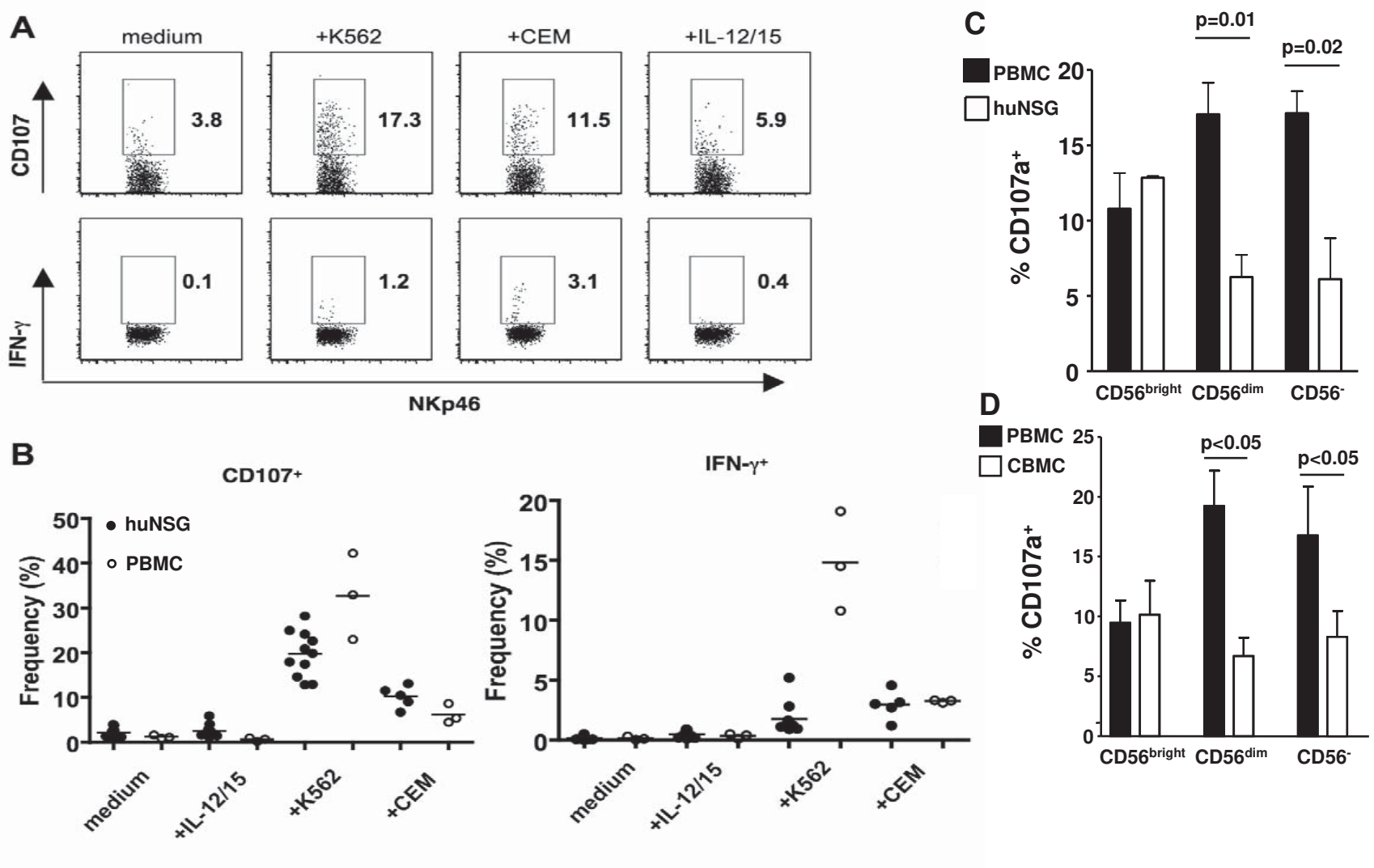
A
medium
+K562
+CEM
+IL-12/15
CD107
IFN-γ
3.8
17.3
11.5
5.9
0.1
1.2
3.1
0.4
NKp46
B
CD107+
IFN-γ+
huNSG
PBMC
Frequency (%)
medium
+IL-12/15
+K562
+CEM
C
PBMC
huNSG
p=0.01
p=0.02
% CD107a+
CD56bright
CD56dim
CD56-
D
PBMC
CBMC
p<0.05
p<0.05
% CD107a+
CD56bright
CD56dim
CD56-

Figure 3

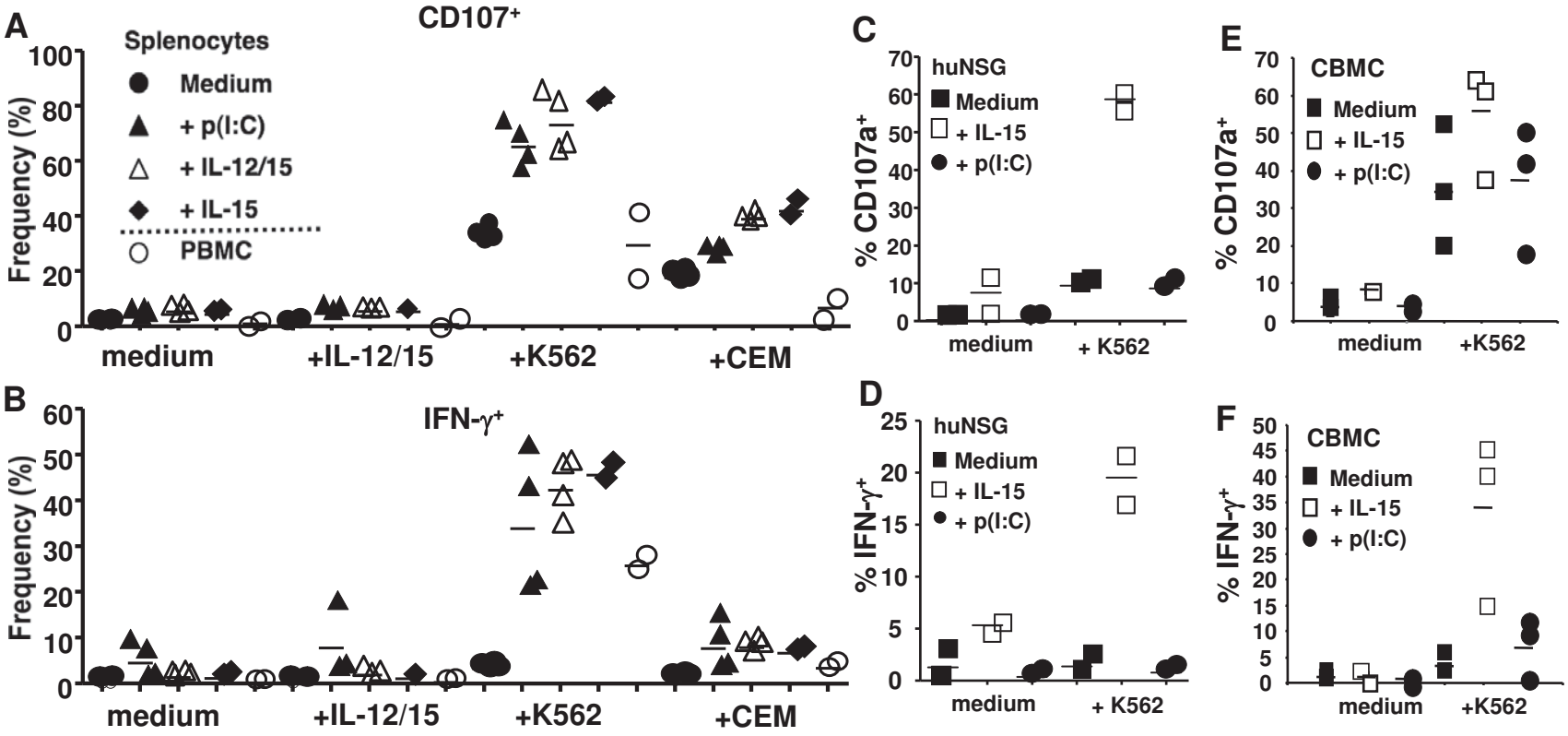
A
CD107+
Splenocytes
Medium
+ p(I:C)
+ IL-12/15
+ IL-15
PBMC
Frequency (%)
medium
+IL-12/15
+K562
+CEM
B
IFN-γ+
Frequency (%)
medium
+IL-12/15
+K562
+CEM
C
huNSG
Medium
+ IL-15
+ p(I:C)
% CD107a+
medium
+ K562
D
huNSG
Medium
+ IL-15
+ p(I:C)
% IFN-γ+
medium
+ K562
E
CBMC
Medium
+ IL-15
+ p(I:C)
% CD107a+
medium
+K562
F
CBMC
Medium
+ IL-15
+ p(I:C)
% IFN-γ+
medium
+K562

Figure 4

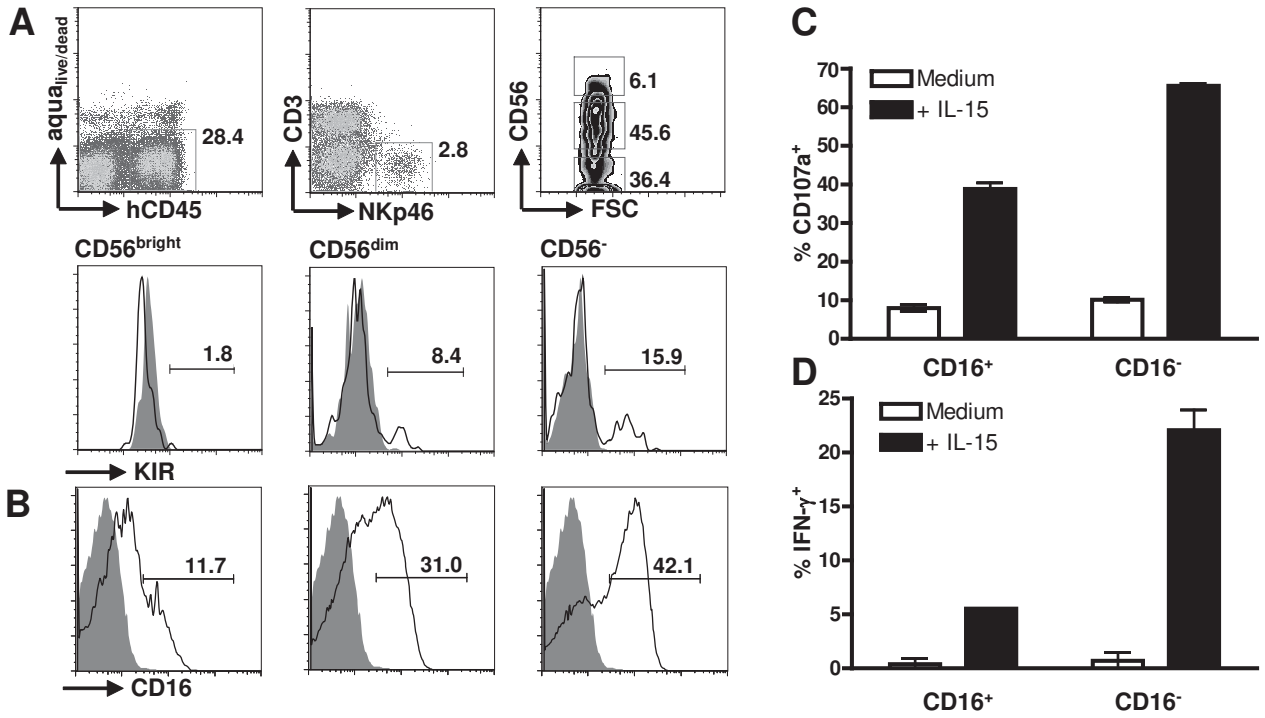
A
aqua live/dead
28.4
hCD45
CD3
2.8
NKp46
CD56
6.1
45.6
36.4
FSC
CD56bright
CD56dim
CD56-
1.8
8.4
15.9
KIR
B
11.7
31.0
42.1
CD16
C
Medium
+ IL-15
% CD107a+
70
60
50
40
30
20
10
0
CD16+
CD16-
D
Medium
+ IL-15
% IFN-γ+
25
20
15
10
5
0
CD16+
CD16-

Figure 5

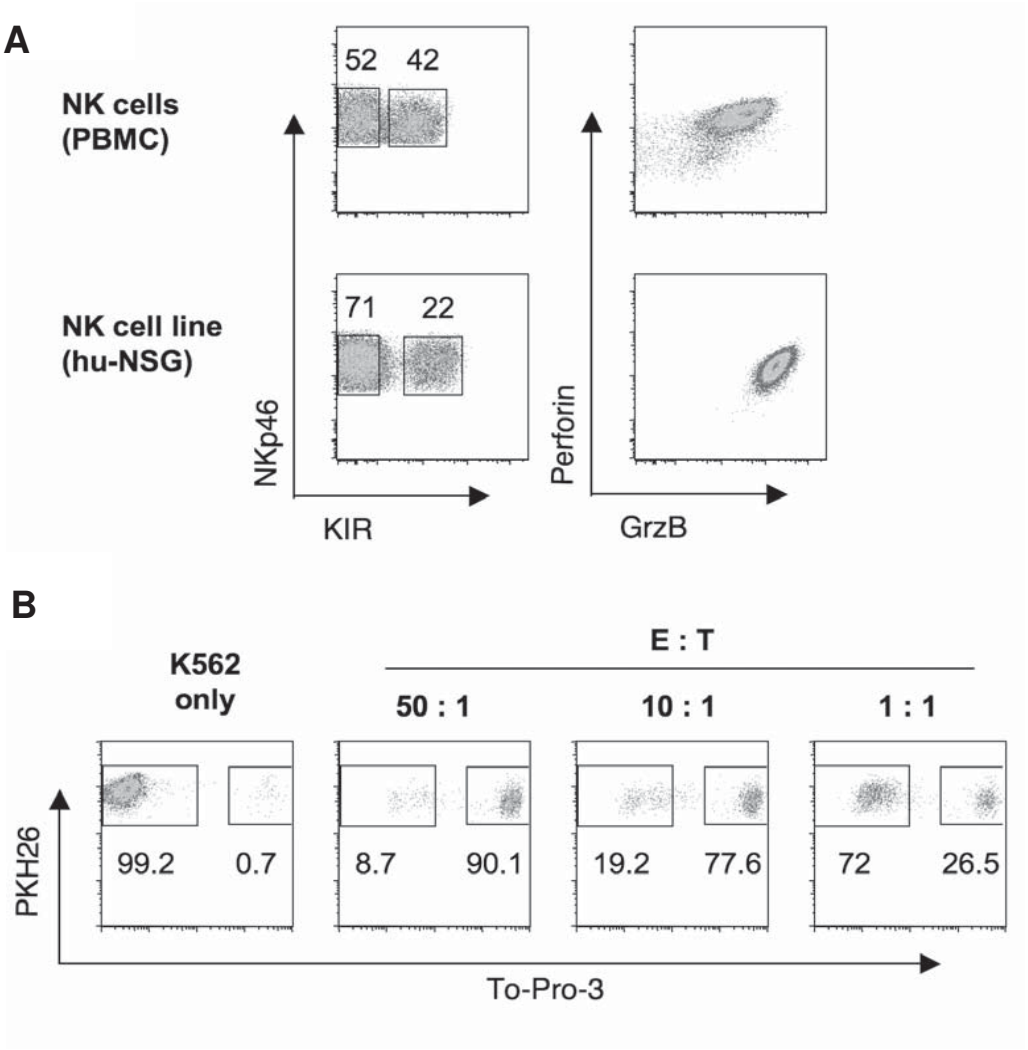
A
NK cells
(PBMC)
52
42
NK cell line
(hu-NSG)
71
22
NKp46
KIR
Perforin
GrzB
B
K562
only
E : T
50 : 1
10 : 1
1 : 1
99.2
0.7
8.7
90.1
19.2
77.6
72
26.5
PKH26
To-Pro-3

Figure 6

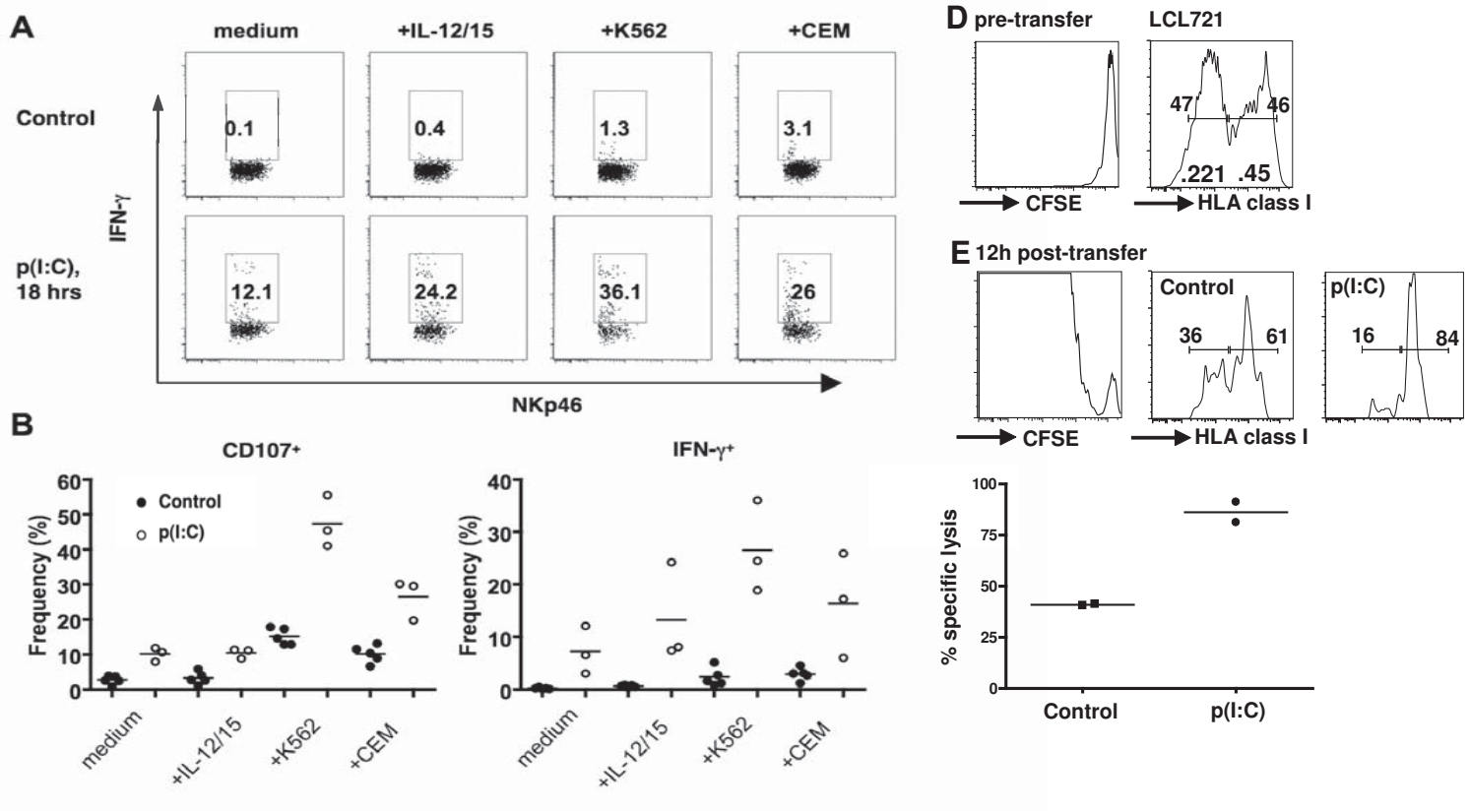
A
medium
+IL-12/15
+K562
+CEM
Control
p(I:C), 18 hrs
IFN-γ
NKp46
0.1
0.4
1.3
3.1
12.1
24.2
36.1
26
B
CD107+
IFN-γ+
Control
p(I:C)
Frequency (%)
medium
+IL-12/15
+K562
+CEM
D pre-transfer
LCL721
CFSE
HLA class I
47
46
.221
.45
E 12h post-transfer
Control
p(I:C)
36
61
16
84
% specific lysis
Control
p(I:C)

Figure 7